JOURNAL OF CHEMICAL EDUCATION

pubs.acs.org/jchemeduc

Laboratory Experiment

Study of Electrochemical Mechanisms Using Computational Simulations: Application to Phenol Butylated Hydroxyanisole

Valeria Tapia Mattar, Edgardo Maximiliano Gavilán-Arriazu,* and Sergio Antonio Rodriguez*

Cite This: https://doi.org/10.1021/acs.jchemed.1c01230

Read Online

ACCESS | Metrics & More | Article Recommendations | Supporting Information

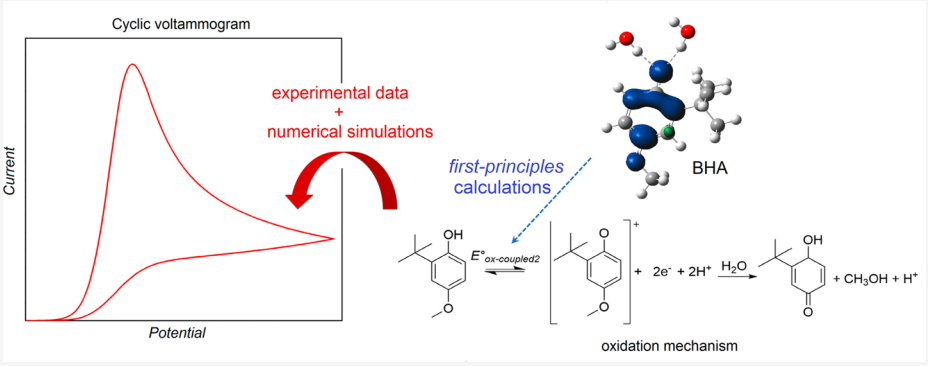

ABSTRACT: Understanding the physicochemical properties of organic compounds with potential biological uses is central in current research topics. Thus, students must pursue the integration of different fields of chemistry to obtain and understand the physicochemical parameters that characterize the mechanism of action of key organics compounds. This proposal encourages the use of computational chemistry in conjunction with experimentally reported data, to study the general oxidation mechanism of a commonly used commercial antioxidant, phenol butylated hydroxyanisole (BHA). The present methodology will let students handle and analyze both thermodynamic and kinetic information. Results allow proposing all possible BHA oxidation paths and concluding which one of them is the most likely to occur, based on the evaluation of theoretical and experimental data. Overall, students are allowed to experience a systematic approach to studying the physicochemical behavior of one organic molecule within a research-like environment.

KEYWORDS: *Upper-Division Undergraduate, Organic Chemistry, Computed-Based Learning, Molecular Properties/Structure*

INTRODUCTION

In the teaching of organic chemistry, the use of computational methods helps to illustrate trends in the properties and reactivity of molecules. One of the most important processes studied in bioorganic molecules is their oxidation mechanism which allows understanding their bioactivity. The main thermodynamic parameters which describe these oxidation reactions are the standard oxidation potential ($E°$) and pK_a values of involved molecules. These parameters could be computationally calculated in very good agreement with experimental data using computational chemistry. As an example, the oxidation mechanism of ascorbic acid was studied calculating the pK_a and reduction potentials of the main molecules involved in its mechanism using the density functional theory (DFT) method B3LYP/6-31+G(d,p) and CBS-QB3 levels of theory with the SMD implicit solvent model and explicit waters.[1]

Electrochemical techniques have the advantage of linking thermodynamics and the kinetics aspects of a redox couple. This is the case of cyclic voltammetry (CV) which is applied in several fields of science, such as the development of biosensors,[2] sensing and detection of antioxidants,[3] underpotential deposition,[4] and batteries technology[5] (a brief description in the Supporting Information). Much of the basic theory of voltammetric methods allows the discernment of a particular mechanism and acquisition of kinetic and thermodynamic information through the analysis of experimental CV and its digital simulations.[6−8]

The present lecture is based on the study of one antioxidant mechanism. Food antioxidant additives represent an important class of compounds that are widely used in the food industry to preserve and improve the foodstuff characteristics such as color, flavor, and nutritional value, among others.[9] Synthetic

Received: December 14, 2021
Revised: January 5, 2022

antioxidants, in particular phenolic ones, are usually applied for oily and fatty products to prevent oxidative processes caused by lipid peroxidation.[10] The most common preserving additives are sterically hindered phenols butylated hydroxyanisole (BHA), *tert*-butyl hydroquinone (TBHQ), butylated hydroxytoluene (BHT), and mixtures of them.

The electrochemical behavior of BHA, TBHQ, and BHT was studied by cyclic voltammetry (CV) in numerous works.[11−21] While most of them seek to obtain analytical information, we have found a few examples where physicochemical aspects are addressed in depth. This is so because the study of the oxidation of phenol and its derivates is challenging, both experimentally and theoretically, due to multiple side chain reactions that suffer reactive intermediates to give an irreversible oxidation mechanism. For example, since the half-peak potential, $E_{1/2}$ (mean value between oxidation and reduction potential peaks used to calculate $E°$), is not always available, the potential peak (E_p) is generally used as an approximation. In this context, computational approaches take relevance.

The main goal of this physical chemistry Laboratory Experiment is that students can use two different simulations methods, DFT calculations, and CV simulations, to study and analyze the thermodynamics and kinetics of BHA, to understand its oxidation mechanism.

The following concepts can be introduced to students:

- The use of *first-principles* calculations to study the thermodynamics of BHA and its oxidation mechanism.
- The implementation of cyclic voltammetry simulations to obtain thermodynamic and kinetic information by comparison with experimental voltammograms.
- The use of DFT and CV simulations in a complementary way to study the oxidation mechanism of BHA.

DENSITY FUNCTIONAL THEORY CALCULATIONS

Density functional theory (DFT) is a type of electronic structure calculation. The main practical difficulty for all electronic structure theories is the proper treatment of electron−electron interactions in species that contain two or more electrons. DFT requires the computation of the total electron density. However, this simulation technique generally uses a wave function to compute some parts of the energy and the electron density to compute other parts of the energy.[22] Modern implementations of DFT can provide accurate calculations at a low computational cost.[23] This fact has led to a steady increase in the use of density functional theory for the study of larger molecules.

Students shall utilize DFT to calculate the energy of all molecules represented in the BHA mechanism. Calculations were performed by the Gaussian 09 rev. E01 series of programs using the hybrid density functional B3LYP, basis sets 6-31+G(d,p), and the SMD implicit solvation model.[24−26] The calculations could be adapted for the use of any available electronic structure software. Slight differences in free energies calculations could be found depending on the selection of basis set and functional and software package choice. We encourage students to use the same basis set and functional to reproduce the results reported.

For BHA, students must (i) build the input molecular geometry, (ii) obtain the lowest-energy geometric configuration performing a "geometry optimization" for geometrical isomers, and (iii) perform a frequency calculation on the optimized geometries to obtain important thermodynamic corrections and to verify the identity of each geometry as an energetic minimum by the absence of imaginary frequencies (Figure 1).[27] Finally, the most stable structure is used to build

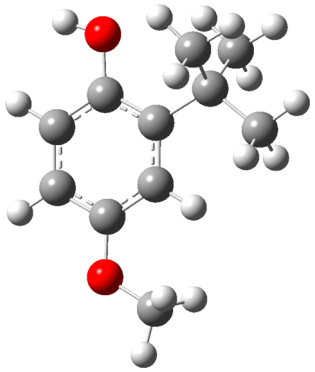

Figure 1. DFT optimized structure of BHA.

the input of the parent molecules radical cation, radical, anion, dication, and cation. Geometry optimizations and frequency calculations must be done for each parent molecule (the coordinates of the optimized molecules are provided in "Coordinates" in the Supporting Information). This sequence of calculations is representative of the general procedure used in routine computational investigations and provides students with a good introduction to the application of electronic structure programs.

Using the Gibbs free energies obtained from calculations the students must calculate pK_a and $E°$ for the oxidation process.

The pK_a calculation was based on the proton dissociation reaction shown in eq 1.[26,28] The pK_a of molecule HA (generic acid) was calculated according to eq 2, where G^*_{aq,A^-} and $G^*_{aq,HA}$ are the standard free energy of deprotonated and protonated species, respectively, calculated directly in aqueous solution at 298.15 K.

$$HA_{aq} \xrightarrow{\Delta G^*_{aq}} A^-_{aq} + H^+_{aq} \tag{1}$$

$$pK_a = \frac{\Delta G^*_{aq}}{2.303RT} = \frac{G^*_{aq,A^-} + G^*_{aq,H^+} - G^*_{aq,HA}}{2.303RT} \tag{2}$$

The Gibbs free energy of a proton in the aqueous phase is calculated using the following equations.[26,28]

$$G^*_{aq,H^+} = G^\circ_{g,H^+} + \Delta G^*_{aq,solv\,H^+} + \Delta G^{1\,atm\rightarrow 1\,M} \tag{3}$$

G°_{g,H^+} = −6.287 kcal/mol at 298 K.[28] $\Delta G^*_{aq,solv\,H^+}$ = −265.9 kcal/mol is the aqueous phase solvation free energy of the proton, taken from the literature.[29] $\Delta G^{1atm\rightarrow 1M} = RT$ (24.46) = 1.89 kcal/mol is a correction term for the change in a standard state of 1 atm to 1 mol/L. The symbols * and ° denote the standard state of 1 mol/L and 1 atm, respectively.

$$G^*_{aq,A^-} = E + \mathrm{ZPVE} + \begin{pmatrix}\text{electronic and thermal}\\ \text{free energy correction}\end{pmatrix}$$

$$G^*_{aq,HA} = E + \mathrm{ZPVE} + \begin{pmatrix}\text{electronic and thermal}\\ \text{free energy correction}\end{pmatrix}$$

https://doi.org/10.1021/acs.jchemed.1c01230
J. Chem. Educ. XXXX, XXX, XXX−XXX

where E = electronic energy for A^- or HA obtained by structure optimization; ZPVE = zero-point vibrational energy in solution.

For a reduction reaction,

$$A_{aq} + ne^- \xrightarrow{\Delta G^*_{red(aq)}} A^{n-}_{aq} \quad (4)$$

the standard reduction potential is

$$E^\circ_{red(aq)} = -\frac{\Delta G^*_{red(aq)}}{nF} - SHE \quad (5)$$

where $\Delta G^*_{red(aq)}$ is the Gibbs free energy of the reduction in standard conditions, n is the number of electrons transferred in the process, F is Faraday's constant (23.06 kcal (mol V)$^{-1}$), and SHE is the absolute potential of the standard hydrogen electrode (4.281 V).[29,30] The Gibbs free energy for reduction is

$$\Delta G^*_{red(aq)} = G_{aq}(A^{n-}) - G_{aq}(A) - nG^\circ_g(e^-) \quad (6)$$

where $G^\circ_g(e^-)$ is the gas-phase free energy of one electron. At 298 K, the gas phase Gibbs energy of an electron is $G^\circ_g(e^-)$ = 0.867 kcal/mol and is obtained from the literature values of $H^\circ_g(e^-)$ = 0.752 kcal/mol and $S^\circ_g(e^-)$ = 5.434 kcal/(mol K).[31]

All pK_a and E calculations were summarized in an Excel file "BHA.xlsx" in Supporting Information.

CYCLIC VOLTAMMETRY: MECHANISMS AND SIMULATIONS

During a voltammetric experiment, different physicochemical sources can modify the current response when applying a potential ramp, namely, coupled chemical reactions, multielectron transfer steps, and kinetic limitations. A simple way to extract all this valuable information is by fitting experimental voltammograms with numerical simulations, given a mechanism that correctly describes the reaction and implementing the fundamental equations of electrochemistry.

The notation used in this work for an electron transfer step is E, while homogeneous chemical reactions are represented with the letter C. The simplest mechanism in an electrochemical reaction is a single electron transfer (E), as shown in Figure 2a. For an oxidation reaction, this is

$$A \underset{k_b}{\overset{k_f}{\rightleftharpoons}} B + ne^- \quad (7)$$

In this equation k_f and k_b are the rate constants for the forward and backward reactions, respectively. These constants can be calculated with the Butler–Volmer scheme:[8]

$$k_f = k^0\, e^{(1-\alpha)nF(E-E^0)/RT} \quad (8)$$

$$k_b = k^0\, e^{-\alpha nF(E-E^0)/RT} \quad (9)$$

$$i = nFA(c_{A,0}k_b - c_{B,0}k_f) \quad (10)$$

where k^0 is the standard heterogeneous rate constant, E is the working electrode potential, E^0 is the standard potential (eq 5), R is the universal gas constant and T is the temperature. Then, i is the current response, α is the transfer coefficient, A is the electrode surface area and $c_{A,0}$ and $c_{B,0}$ are the concentration of species A and B at the electrode surface, respectively. For example, the variations on the sweep rate (v) or k^0 yield

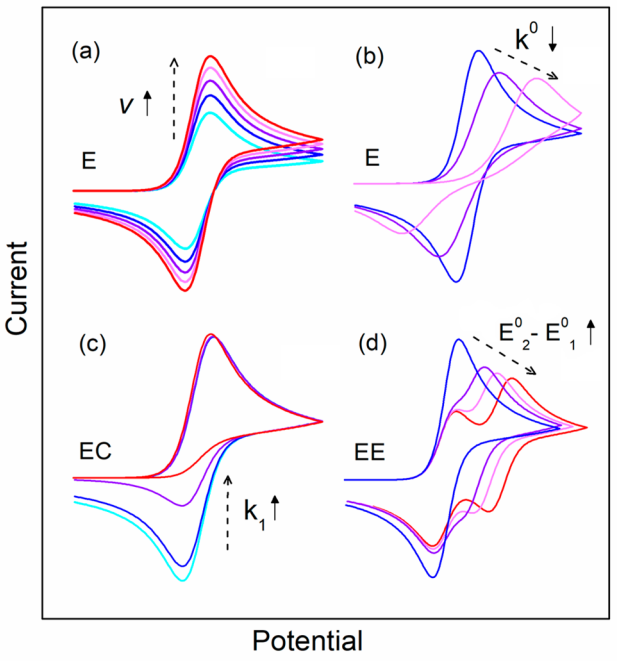

Figure 2. Illustrative examples of voltammetric general responses for (a) a single electron transfer (E) when increasing sweep rate, in arbitrary units (au); (b) a single electron transfer (E) when varying k^0 (au); (c) EC reaction when varying k_1 (au); (d) EE reaction varying E^0_1 and E^0_2 (au). Simulations were performed with dimensionless coordinates as defined in ref, 7 so solutions are independent of bulk concentration, diffusion coefficient, and electrode dimensions. The solid black arrows indicate if the parameter increases (arrow pointing up) or decreases (arrow pointing down). The behavior of the current response from these changes is highlighted with a broken arrow.

different current responses, as shown in Figure 2 panels a and b, respectively.

The EC reaction (eq 11) consists of a redox step (E) followed by a chemical reaction (C).

$$A \underset{k_b}{\overset{k_f}{\rightleftharpoons}} B + ne^-$$
$$B \xrightarrow{k_1} Y \quad (11)$$

In this case, step C is considered irreversible, so the rate of the chemical reaction (determined by the homogeneous rate constant,k_1), compared to the rate of the electron transfer reaction, will determine the height of one of the current peaks, as shown in Figure 2c.

Also, multiple electron transfer processes, such as two consecutive electron transfer steps (EE mechanism), may occur (eq 12).

$$A \underset{k_{b,1}}{\overset{k_{f,1}}{\rightleftharpoons}} B + n_1e^-, \quad E^0_1$$
$$B \underset{k_{b,2}}{\overset{k_{f,2}}{\rightleftharpoons}} Y + n_2e^-, \quad E^0_2 \quad (12)$$

The shape of the voltammogram in this case will strongly depend on the thermodynamics of each reaction. If the second process is more favored compared with the first ($E^0_1 > E^0_2$), a single voltammetric peak will be observed in each potential sweep. Conversely, if the first peak is more favored than the

https://doi.org/10.1021/acs.jchemed.1c01230
J. Chem. Educ. XXXX, XXX, XXX−XXX

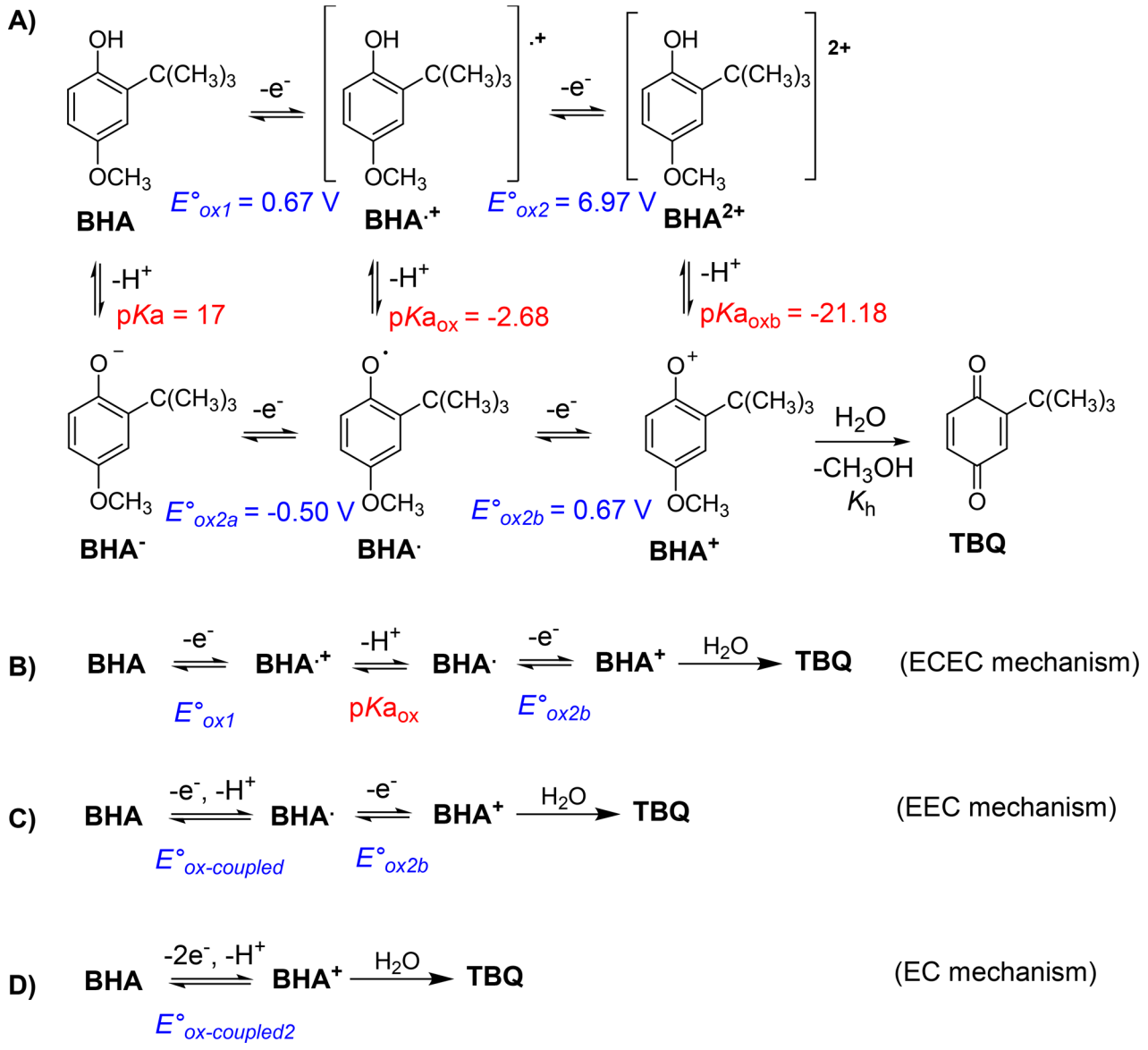

Figure 3. (A) pK_a and $E°$ values represented in the step-by-step BHA oxidation mechanism. (B–D) Possible coupled electrochemical mechanisms.

second ($E_1^0 < E_2^0$), the presence of one or two peaks will depend on how close the standard potentials are. The latter condition is represented in Figure 2d.

Similar to the mechanisms presented above as an introduction, other reactions may occur in an electrochemical environment, such as CE, EEC, and CEE.

The fundamental equations and the resolution of partial differential equations with the finite differences method are provided in "Simulations" in the Supporting Information. An introduction to the mathematical modeling in electrochemistry can be found in ref 32. Also, in this regard, we recommend turning to the educational work of Brown,[6] that served as the basis for our CV codes written in C++. Additionally, we can also cite the work of Wang et al.[33] to develop and use a voltammetric simulator and a Web site for simulating cyclic voltammetry experiments (http://limhes.net/ecsim/).

The fitting of the experimental voltammogram can be made with computational programs[34] starting from guessed values. However, students need to exercise fitting the curves manually, since this gives a useful tool to learn the basic concepts of electrochemistry by handling them. We recommend a bibliographic search of the unknown parameters before the fitting step, to get a reliable starting point.

RESULTS

DFT Calculations

The BHA oxidation mechanism could be analyzed into individual electron transfer and proton transfer steps to understand the fundamental electrochemistry of the global process (Figure 3A). Each electron transfer process is characterized by a standard oxidation potential ($E°_{ox1}$, $E°_{ox2}$, $E°_{ox2a}$, and $E°_{ox2b}$) and each acid–base process by a pK_a value (pK_a, p$K_{a\,ox}$, and p$K_{a\,oxb}$) (Figure 3A). Finally, if a chemical reaction is coupled, it can be described by the hydrolysis constant, K_h, to form *tert*-butyl-*p*-benzoquinone (TBQ) (Figure 3A).

To compute the pK_a and $E°$ values proposed in Figure 3, the water-phase calculated electronic and thermal free energies ($G_{(aq)}$) for BHA and parent molecules (in energy units of Hartree) are listed in Table 1. To convert to energy units of

https://doi.org/10.1021/acs.jchemed.1c01230
J. Chem. Educ. XXXX, XXX, XXX–XXX

Table 1. DFT Calculated Energies for Optimized Geometries

Structure	$G_{(aq)}$/(Hartrees)	$G_{(aq)}$/(kcal mol^{-1})
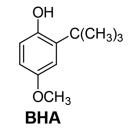 BHA	-579.083423	-363380
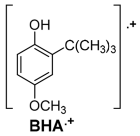 $BHA^{\cdot+}$	-578.892056	-363260 225
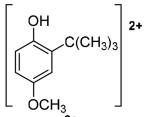 BHA^{2+}	-578.660338	-363115
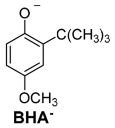 BHA^{-}	-578.615713	-363087
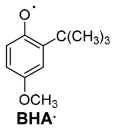 $BHA^{\cdot}$	-578.467143	-362994
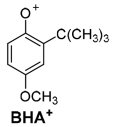 BHA^{+}	-578.275622	-362873

kcal mol^{-1} the following factor is used, 1 hartree = 627.5095 kcal mol^{-1}. All results are summarized in the Supporting Information. The oxidation potentials were referred to the Ag/AgCl electrode by the sum of −0.,223 V to the values obtained with eq 5.

The experimental pK_a of BHA was not reported in the bibliography but must be similar to the pK_a of phenol (10),[35] 2-*t*-butylphenol (11.24),[36] 2,4-di-*t*-butylphenol (11.57),[36] and BHT (12.23).[37] The deprotonation reaction of BHA presents a calculated pK_a of 17 (Figure 3A), this value being higher than expected. This is so because the BHA anion has more spread-out electron densities than neutral BHA; the calculation of solvation energies of anion species needs more complex treatment and this is outside the goal of the present manuscript.[26] The pK_a for oxidized species $BHA^{\cdot+}$ and BHA^{2+} (p$K_{a\,ox}$ and p$K_{a\,oxb}$) are negatives indicating that they are strong acids (the proton transfer reactions are thermodynamically favored).

The first electron transfer has an E°_{ox1} lower than the second, E°_{ox2}, which implies that the first oxidation step is a single electron transference and not two consecutive electron processes (Figure 3A). If this reaction was made from BHA^{-}, an anion, the oxidation potential (E°_{ox2a}) will be more favored; but this electron transfer is ruled by the pH. After, the deprotonation of $BHA^{\cdot+}$ to produce BHA·, a new electron transference is possible with an E°_{ox2b} equal to E°_{ox1} which allows the formation of BHA^{+} (Figure 3A). In conclusion, at physiologic pH (approximately 7), the oxidation of BHA could be described as a two-electron and one proton transfer process (Figure 3B). On the other hand, due to the high acidity of BHA^{+} it is possible to propose a first step involving a coupled electron and proton transfer ($E^{\circ}_{ox\text{-}coupled}$) followed by a second electron transference (Figure 3C). Finally, due to $E^{\circ}_{ox1} = E^{\circ}_{ox2b}$, the student could state the possibility of a two-electron and one proton transference described by $E^{\circ}_{ox\text{-}coupled2}$ (Figure 3D). All these mechanisms are coupled with a hydrolysis reaction with water to produce TBQ.

The oxidation potentials of coupled electron and proton transfers could be calculated using the proton enthalpy in eq 6; being $E^{\circ}_{ox\text{-}coupled}$ = 0.51 V and $E^{\circ}_{ox\text{-}coupled2}$ = 0.59 V. The BHA oxidation mechanism has been studied using CV. The anodic peak potential reported was in the range of 0.44−0.60 V in aqueous systems, neutral to acidic pH, referenced to Ag/AgCl electrode, a working glassy carbon electrode, and carbon composite electrode, and different supporting electrolytes.[11,18,20,21,38] Both, $E^{\circ}_{ox\text{-}coupled}$ and $E^{\circ}_{ox\text{-}coupled2}$ are in good agreement with the reported values.

At this point, it is necessary to complement these results with the CV section.

Cyclic Voltammetry

In this section, the students will explore the kinetics and thermodynamics of BHA by using CV simulations. For this task, the oxidation mechanisms proposed for BHA in the section DFT Calculations (Figures 3C,D) are used for modeling numerical simulations. As observed, these mechanisms are EEC and EC. We will focus first on EC and then on EEC. Finally, we will contrast the oxidation potentials obtained with DFT with data obtained from the voltammetric analysis.

The experimental cyclic voltammogram was taken from Freitas and Fatibello-Filho.[38] The authors reported working with a sweep speed of 50 mV·s^{-1} using a three part electrode with a composite carbon electrode (particulate carbon with solid paraffin) as the working electrode and Ag/AgCl as the reference electrode, thus all potentials are referred to Ag/AgCl; and a platinum counter electrode. The cell was filled with 0.10 M of KNO_3 in 10% of C_2H_5OH as the support electrolyte, at pH 6.7, and a BHA concentration of 2×10^{-8} mol/cm^3. It was necessary to extract the solvent response to discard sources that affect the current response that were not considered in the theoretical model, since simulations only consider the current given by the redox reaction (pure faradaic current).

Because of the challenges of studying phenol derivates from a theoretical point of view, as commented in the introduction, errors of 50 to 150 mv in computationally E^0 are generally admissible.[39,40] Also, several works have informed that less than 100 mV is a suitable quantity;[39,41,42] so, we will take this last value as acceptance criteria.

(a). EC Mechanism (2 Electrons and 1 Proton Transfer). We propose three different fits, EC-1, EC-2, and EC-3 (Table 2 and Figure 4), using 700 points in time and 100 points in space for the simulation grid. The bulk concentration of BHA (c_{BHA}) and sweep rate (ν) were those from experimental conditions. The diffusion coefficient was tacked as a fixed value. We used $D = 8.0 \times 10^{-7}$ cm^2/s, which is close to that obtained for BHA experimentally with a bare glassy carbon electrode (7.28×10^{-7} cm^2/s).[43] Although the electrodes from the last cite and that from Freitas and Fatibello-Filho[38] are not the same, both are made with carbonaceous materials, and thus, we can safely presume that for bare electrodes there will not be large differences. D will be

https://doi.org/10.1021/acs.jchemed.1c01230
J. Chem. Educ. XXXX, XXX, XXX−XXX

Table 2. Experimental Parameters and Values Used to Fit the Experimental BHA Voltammogram Considering an EC Mechanism

parameter	EC-1	EC-2	EC-3
c_{BHA} [mol/cm^3]	2.0×10^{-8}	2.0×10^{-8}	2.0×10^{-8}
v [mV/s]	50	50	50
n	2	2	2
D [cm^2/s]	8.0×10^{-7}	8.0×10^{-7}	8.0×10^{-7}
k_1 [s^{-1}]	10	10	10
A [cm^2]	0.29	0.32	0.32
α	0.3	0.5	0.7
E^0 [V]	0.490	0.523	0.545
k^0 [cm/s]	5.0×10^{-5}	5.0×10^{-4}	1.5×10^{-3}

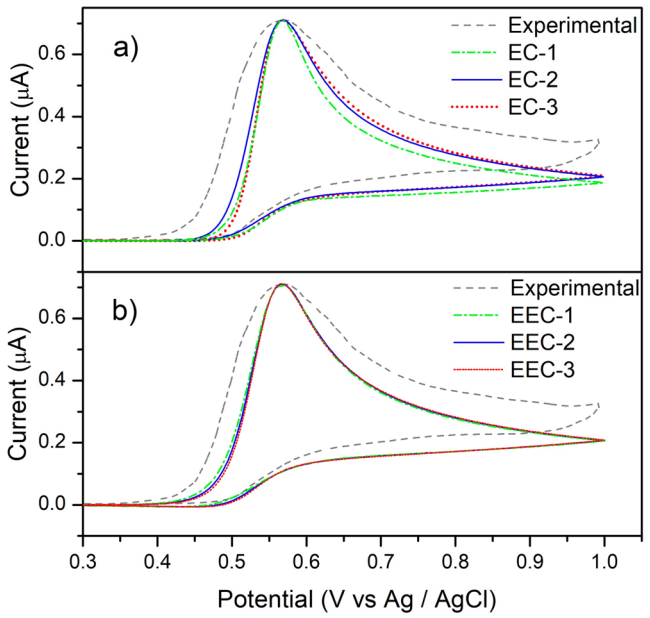

Figure 4. (a) EC numerical simulations with parameters of Table 2 and BHA voltammogram from ref 38. The names of the fits are marked in the figure. (b) EEC numerical simulations with parameters of Table 3 and BHA voltammogram from ref 38. The names of the fits are marked in the figure. Experimental voltammogram reproduced with permission from ref 38. Copyright 2010 Elsevier.

the same for all species. The homogeneous rate constant, k_1 = 10 s^{-1}, was also taken as a fixed value. We found that the last quantity is high enough to consume most of the oxidation products to simulate an irreversible chemical step C. The rest of the quantities were considered as fitting variable parameters.

As observed in Figure 4a, the three fits present reasonable responses, with small differences. In most systems α lies between 0.3 and 0.7,[8] so we used 0.3, 0.5, and 0.7. In each case, different E^0 and k^0 were obtained. As observed, as α increases, higher values of E^0 and k^0 are needed to fit the experimental curve. Regarding a heterogeneous charge transfer constant, we did not find experimental determinations of k^0 for BHA in the literature. So, we will use $k^0_{phenol} = 7 \times 10^{-4}$ cm/s[44] as a reference point. It is expected that $k^0_{BHA} > k^0_{phenol}$ since the BHA substituents (*t*-butyl and *O*-methyl) stabilizes the oxidation products with respect to the phenol oxidation products.

The students can also evaluate the charge transfer reversibility with eq 13, which depends on kinetic parameters and operating conditions.[8,45]

$$\Lambda = k^0(RT/nFDv)^{1/2} = \begin{cases} \Lambda \geq 15 & \text{reversible} \\ 15 > \Lambda > 10^{-2(1+\alpha)} & \text{quasi-reversible} \\ \Lambda \leq 10^{-2(1+\alpha)} & \text{irreversible} \end{cases} \quad (13)$$

According to this definition, all fits are under quasi-reversibility conditions.

(b). EEC Mechanism (2 Steps of 1 Electron Transfer and 1 Proton Transfer). For this mechanism, we will follow the same procedure and fixed values of D, α, k_1, c_{BHA} and v as in the previous case. 7000 points in time and 300 points in space were needed to perform numerical simulations. We will assume that the charge transfer constants for the consecutive E charge transfer steps are the same ($k^{0(1)} = k^{0(2)} = k^0$). We will also take that α is the same for both redox steps and that $E^0_1 = E^0_2 = E^0$, since the theoretical values calculated with DFT are close. All values used in the simulations are shown in Table 3.

Table 3. Experimental Parameters and Values Used to Fit the Experimental BHA Voltammogram Considering an EEC Mechanism

parameter	EEC-1	EEC-2	EEC-3
c_{BHA} [mol/cm^3]	2.0×10^{-8}	2.0×10^{-8}	2.0×10^{-8}
v [mV/s]	50	50	50
$n^{(1)}$	1	1	1
$n^{(2)}$	1	1	1
D [cm^2/s]	8.0×10^{-7}	8.0×10^{-7}	8.0×10^{-7}
k_1 [s^{-1}]	10	10	10
A [cm^2]	0.32	0.32	0.32
α	0.3	0.5	0.7
E^0 [V]	0.5	0.527	0.538
k^0 [cm/s]	1.5×10^{-3}	3.4×10^{-3}	5.4×10^{-3}

As observed in Figure 4b the current response for EEC is similar to that of EC, but in the present case, the simulated curves are similar to each other. The similarity between the current responses of EEC-1, EEC-2, and EEC-3 compared to EC-1, EC-2, and EC-3 can be understood by comparing the parameters in Table 3 and Table 2. As observed, different k^0 and E^0 are more likely in the two-step reaction. Also, in the three EEC cases k^0 is in the order of 10^{-3} cm/s, that is, larger than that of phenol; while in the EC reaction, EC3 is the only fit that exceeds the phenol value. Students can check with eq 13 the quasi-reversibility nature in all cases.

In the Supporting Information, Figure S3, we show that a difference of 173 mV between E^0_1 and E^0_2 must be observed to well distinguish a pair of peaks.

One last comment to these last sections: Although the coincidences between experimental and theoretical curves are acceptable, different peak widths are observed. This is so because we have not considered the influence of capacitive charging current in digital simulations,[8] apart from minor numerical sources of error. To account for nonfaradaic sources, the work of Orlik is a good option.[46] Otherwise, slower scan rates than 50 mV/s (5 mV/s or less) are needed to reduce experimental charging contributions as much as possible. This is a useful consideration in the case of performing experimental measurements.

https://doi.org/10.1021/acs.jchemed.1c01230
J. Chem. Educ. XXXX, XXX, XXX−XXX

Analyzing DFT and Cyclic Voltammetry Results

In this section, the calculated DFT potentials (E^0) for EC and EEC mechanisms are used as input values in eqs 8 and 9, for simulating CV. According to the section DFT Calculations, the oxidative potential calculated for the EC mechanism is 0.59 V, while those for EEC are E_1^0 = 0.67 V and E_2^0 = 0.67 V.

At this stage, it is important to note that corrections need to be made to properly compare experimental and theoretical E^0. Students should distinguish that DFT calculations were performed for pH = 0, since experimental conditions present pH = 6.7. As observed in several experimental works, pH changes may cause appreciable differences in the equilibrium potentials,[47] so this factor must be considered in the analysis.

An easy way to adjust the experimental potential to pH = 0 is by plotting an anodic potential vs pH curve. The work[38] informs a slope of 29.5 mV/pH for BHA, so this means that the experimental potentials need to be corrected by +198 mV to shift experimental E^0 from pH = 6.7 to pH = 0.

Experimental and simulated voltammograms are shown in Figure 5. As observed qualitatively by comparing potential peaks, the best approach is that of EEC-1. EC peak potentials look far from the experimental case, more than 100 mV.

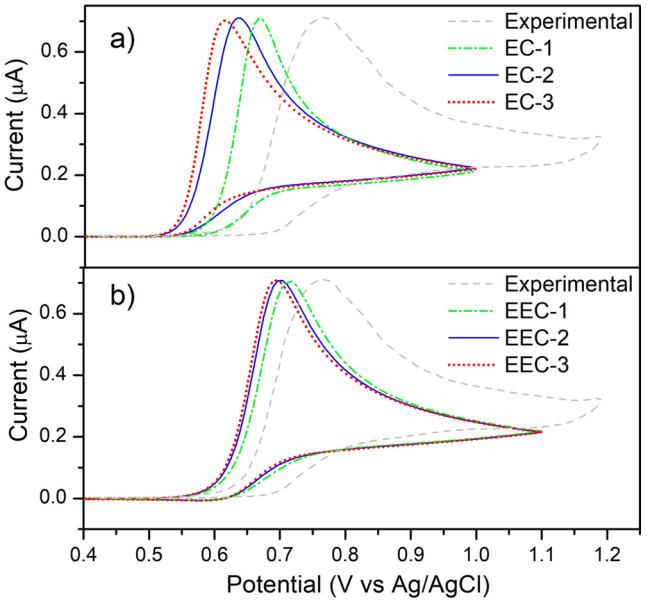

Figure 5. (a) EC numerical simulations using E^0 = 0.59 V and BHA voltammogram from ref 38; experimental curve has been shifted to the value corresponding to pH = 0. The names of the fits are marked in the figure. (b) EEC numerical simulations using calculated $E^0 = E_1{}^0 = E_2{}^0$ = 0.67 V and BHA voltammogram from ref 38, experimental curve has been shifted to the value corresponding to pH = 0. Experimental voltammogram reproduced with permission from ref 38. Copyright 2010 Elsevier.

Table 4 shows pH corrected and uncorrected potentials, the theoretical ones, and the resulting difference between the experimental and theoretical oxidative potentials at pH = 0. The colors in the last case emphasize if the difference is minor of 100 mV (green), out of this range (red), or close to the limiting value (orange). As observed, the most appropriate mechanism is EEC, because the potential errors are under 100 mV in all cases. The best approach is that for EEC-1, (<30 mV). This result also coincides with the predictions made that k^0 for BHA must be greater than that of phenol.

Table 4. Experimental E^0 for pH = 6.7 and pH = 0, Theoretical E^0 for EC and EEC Calculated in This Work and Difference between the Experimental (E^0_{exp}) and theoretical (E^0_{theor}) E^0 for pH = 0[a]

Fit name	Experimental-Fitted E^0, pH=6.7 (mV)	Experimental E^0 corrected to pH=0 (mV)	Theoretical E^0, pH=0 (mV)	$\lvert E^0_{exp}-E^0_{theor}\rvert$ pH=0 (mV)
EC-1	490	688	590	98
EC-2	523	721	590	131
EC-3	545	743	590	153
EEC-1	500	698	670	28
EEC-2	527	725	670	55
EEC-3	538	736	670	66

[a]The colors in the last column emphasize if the potential difference is minor (green), major (red), or close (orange) of 100 mV.

CONCLUSION

A pedagogical procedure has been presented in this educational work where students can research redox mechanisms by coupling different simulation techniques. In this regard, we encourage teachers and students to replicate this methodology coupled with an experimental cyclic voltammetry lab, either for BHA or for other organic molecules. The use of experimental information from bibliography, as was done in the present work, is another good option, especially in the framework of CODIV-19 pandemic where attendance to laboratories has been reduced.

DFT calculations allowed students to discuss acid−bases and electrochemistry properties of a common antioxidant. Besides, the students could attribute to the phenol system the BHA properties and analyze how different medium conditions modify its behavior, taking into account also the discussion of the bibliography presented. It is important to remark on the necessity of complementing these calculations with experimental techniques and CV simulations to expand student knowledge about BHA.

Digital voltammetric simulations allowed students to reproduce the response of the experimental BHA voltammogram by using the proposed mechanisms from DFT calculations. Kinetic and thermodynamic information was extracted from these simulations. The EC mechanism was previously suggested, while the occurrence of the EEC mechanism is a proposal of the present work. The EEC mechanism yielded the best results.

ASSOCIATED CONTENT

Supporting Information

The Supporting Information is available at https://pubs.acs.org/doi/10.1021/acs.jchemed.1c01230.

DFT and simulation support (PDF, DOCX)
pK_a and E numerical calculations (XLSX)

AUTHOR INFORMATION

Corresponding Authors

Sergio Antonio Rodriguez − *CONICET, Instituto de Ciencias Químicas, FAyA, UNSE, Santiago del Estero G4200, Argentina;* orcid.org/0000-0002-0904-5817; Email: drsergiorod@gmail.com

Edgardo Maximiliano Gavilán-Arriazu − *Departamento de Química Teórica y Computacional, Facultad de Ciencias*

https://doi.org/10.1021/acs.jchemed.1c01230
J. Chem. Educ. XXXX, XXX, XXX−XXX

Químicas, Universidad Nacional de Córdoba, INFIQC, Córdoba X5000, Argentina; Facultad de Matemática, Astronomía y Física, IFEG-CONICET, Universidad Nacional de Córdoba, Córdoba X5000, Argentina; Email: maxigavilan@hotmail.com

Author

Valeria Tapia Mattar − *CONICET, Instituto de Ciencias Químicas, FAyA, UNSE, Santiago del Estero G4200, Argentina*

Complete contact information is available at: https://pubs.acs.org/10.1021/acs.jchemed.1c01230

Notes

The authors declare no competing financial interest.

■ ACKNOWLEDGMENTS

The authors are grateful to Consejo Nacional de Investigaciones Científicas y Técnicas (CONICET), FONCYT and SECYT UNSE for funding. This work used computational resources from CCAD-UNC, which is part of SNCAD-MinCyT, Argentina.

■ REFERENCES

(1) Tu, Y. J.; Njus, D.; Schlegel, H. B. A Theoretical Study of Ascorbic Acid Oxidation and HOO/O 2- Radical Scavenging. *Org. Biomol. Chem.* **2017**, *15* (20), 4417−4431.

(2) Paz Zanini, V. I.; Gavilán, M.; López De Mishima, B. A.; Martino, D. M.; Borsarelli, C. D. A Highly Sensitive and Stable Glucose Biosensor Using Thymine-Based Polycations into Laponite Hydrogel Films. *Talanta* **2016**, *150*, 646.

(3) Blasco, A. J.; Gonzalez Crevillen, A.; Gonzalez, M. C.; Escarpa, A. Direct Electrochemical Sensing and Detection of Natural Antioxidants and Antioxidant Capacity in Vitro Systems. *Electroanalysis* **2007**, *19* (22), 2275−2286.

(4) Hölzle, M. H.; Retter, U.; Kolb, D. M. The Kinetics of Structural Changes in Cu Adlayers on Au(111). *J. Electroanal. Chem.* **1994**, *371* (1−2), 101−109.

(5) Gavilán-Arriazu, E. M.; Mercer, M. P.; Pinto, O. A.; Oviedo, O. A.; Barraco, D. E.; Hoster, H. E.; Leiva, E. P. M. Numerical Simulations of Cyclic Voltammetry for Lithium-Ion Intercalation in Nanosized Systems: Finiteness of Diffusion versus Electrode Kinetics. *J. Solid State Electrochem.* **2020**, *24*, 3279.

(6) Brown, J. H. Development and Use of a Cyclic Voltammetry Simulator To Introduce Undergraduate Students to Electrochemical Simulations. *J. Chem. Educ.* **2015**, *92* (9), 1490−1496.

(7) Compton, R. G.; Laborda, E.; Ward, K. R. *Understanding Voltammetry: Simulation of Electrode Processes*; World Scientifice: Singapore, 2013.

(8) Bard, A. J.; Faulkner, L. R. *Electrochemical Methods : Fundamentals and Applications*; John Wiley and Sons, 2001.

(9) Shahidi, F.; Ambigaipalan, P. Phenolics and Polyphenolics in Foods, Beverages and Spices: Antioxidant Activity and Health Effects - A Review. *Journal of Functional Foods.* **2015**, *18*, 820.

(10) Bruckner, J. Food Antioxidants. Herausgegeben von B. J. F. Hudson. Elsevier Applied Science, London, NY, 1990, Preis: 56,-L. *Food/Nahrung* **1992**, 1 DOI: 10.1002/food.19920360543.

(11) Lin, X.; Ni, Y.; Kokot, S. Glassy Carbon Electrodes Modified with Gold Nanoparticles for the Simultaneous Determination of Three Food Antioxidants. *Anal. Chim. Acta* **2013**, *765*, 54−62.

(12) Ng, K. L.; Tan, G. H.; Khor, S. M. Graphite Nanocomposites Sensor for Multiplex Detection of Antioxidants in Food. *Food Chem.* **2017**, *237*, 912−920.

(13) Caramit, R. P.; De Freitas Andrade, A. G.; Gomes De Souza, J. B.; De Araujo, T. A.; Viana, L. H.; Trindade, M. A. G.; Ferreira, V. S. A New Voltammetric Method for the Simultaneous Determination of the Antioxidants TBHQ and BHA in Biodiesel Using Multi-Walled Carbon Nanotube Screen-Printed Electrodes. *Fuel* **2013**, *105*, 306−313.

(14) Ziyatdinova, G.; Guss, E.; Budnikov, H. Amperometric Sensor Based on MWNT and Electropolymerized Carminic Acid for the Simultaneous Quantification of TBHQ and BHA. *J. Electroanal. Chem.* **2020**, *859*, 113885.

(15) Caramit, R. P.; Antunes Araujo, A. S.; Fogliatto, D. K.; Viana, L. H.; Goncalves Trindade, M. A.; Ferreira, V. S. Carbon-Nanotube-Modified Screen-Printed Electrodes, a Cationic Surfactant, and a Peak Deconvolution Procedure: Alternatives to Provide Satisfactory Simultaneous Determination of Three Synthetic Antioxidants in Complex Samples. *Anal. Methods* **2015**, *7* (9), 3764−3771.

(16) Ziyatdinova, G.; Os'Kina, K.; Ziganshina, E.; Budnikov, H. Simultaneous Determination of TBHQ and BHA on a MWNT-Brij® 35 Modified Electrode in Micellar Media. *Anal. Methods* **2015**, *7* (19), 8344−8351.

(17) Michalkiewicz, S.; Mechanik, M.; Malyszko, J. Voltammetric Study of Some Synthetic Antioxidants on Platinum Microelectrodes in Acetic Acid Medium. *Electroanalysis* **2004**, *16* (7), 588−595.

(18) dos Santos Raymundo, M.; Marques da Silva Paula, M.; Franco, C.; Fett, R. Quantitative Determination of the Phenolic Antioxidants Using Voltammetric Techniques. *LWT - Food Sci. Technol.* **2007**, *40* (7), 1133−1139.

(19) Tomášková, M.; Chýlková, J.; Jehlička, V.; Navrátil, T.; Švancara, I.; Šelešovská, R. Simultaneous Determination of BHT and BHA in Mineral and Synthetic Oils Using Linear Scan Voltammetry with a Gold Disc Electrode. *Fuel* **2014**, *123*, 107−112.

(20) Wang, P.; Han, C.; Zhou, F.; Lu, J.; Han, X.; Wang, Z. Electrochemical Determination of Tert-Butylhydroquinone and Butylated Hydroxyanisole at Choline Functionalized Film Supported Graphene Interface. *Sensors Actuators, B Chem.* **2016**, *224*, 885−891.

(21) Medeiros, R. A.; Rocha-Filho, R. C.; Fatibello-Filho, O. Simultaneous Voltammetric Determination of Phenolic Antioxidants in Food Using a Boron-Doped Diamond Electrode. *Food Chem.* **2010**, *123* (3), 886−891.

(22) Baseden, K. A.; Tye, J. W. Introduction to Density Functional Theory: Calculations by Hand on the Helium Atom. *J. Chem. Educ.* **2014**, *91* (12), 2116−2123.

(23) Sholl, D.; Steckel, J. A. *Density Functional Theory: A Practical Introduction*; John Wiley & Sons, Inc.: Hoboken, NJ, 2009.

(24) Frisch, M. J.; Trucks, G. W.; Schlegel, H. B.; Scuseria, G. E.; Robb, M. A.; Cheeseman, J. R.; Scalmani, G.; Barone, V.; Mennucci, B.; Petersson, G. A.; Nakatsuji, H.; Caricato, M.; Li, X.; Hratchian, H. P.; Izmaylov, A. F.; Bloino, J.; Zheng, G.; Sonnenberg, J. L.; Hada, M.; Ehara, M.; Toyota, K.; Fukuda, R.; Hasegawa, J.; Ishida, M.; Nakajima, T.; Honda, Y.; Kitao, O.; Nakai, H.; Vreven, T.; Montgomery, J. A., Jr.; Peralta, J. E.; Ogliaro, F.; Bearpark, M.; Heyd, J. J.; Brothers, E.; Kudin, K. N.; Staroverov, V. N.; Kobayashi, R.; Normand, J.; Raghavachari, K.; Rendell, A.; Burant, J. C.; Iyengar, S. S.; Tomasi, J.; Cossi, M.; Rega, N.; Millam, J. M.; Klene, M.; Knox, J. E.; Cross, J. B.; Bakken, V.; Adamo, C.; Jaramillo, J.; Gomperts, R.; Stratmann, R. E.; Yazyev, O.; Austin, A. J.; Cammi, R.; Pomelli, C.; Ochterski, J. W.; Martin, R. L.; Morokuma, K.; Zakrzewski, V. G.; Voth, G. A.; Salvador, P.; Dannenberg, J. J.; Dapprich, S.; Daniels, A. D.; Farkas, O.; Foresman, J. B.; Ortiz, J. V.; Cioslowski, J.; Fox, D. J. *Gaussian 09*, rev. E.01; Gaussian; 2009.

(25) Marenich, A. V.; Cramer, C. J.; Truhlar, D. G. Performance of SM6, SM8, and SMD on the SAMPL1 Test Set for the Prediction of Small-Molecule Solvation Free Energies. *J. Phys. Chem. B* **2009**, *113*, 4538.

(26) Rodriguez, S. A.; Baumgartner, M. T. Betanidin p KaPrediction Using DFT Methods. *ACS Omega* **2020**, *5*, 13751.

(27) Foresman, J. B.; Frisch, Æ. *Exploring Chemistry with Electronic Structure Methods*, 3rd ed.; Gaussian, Inc.: Wallingford, CT, 2015.

(28) Thapa, B.; Schlegel, H. B. Improved PKa Prediction of Substituted Alcohols, Phenols, and Hydroperoxides in Aqueous Medium Using Density Functional Theory and a Cluster-Continuum Solvation Model. *J. Phys. Chem. A* **2017**, *121* (24), 4698−4706.

(29) Isse, A. A.; Gennaro, A. Absolute Potential of the Standard Hydrogen Electrode and the Problem of Interconversion of Potentials in Different Solvents. *J. Phys. Chem. B* **2010**, *114*, 7894.
(30) Truhlar, D. G.; Cramer, C. J.; Lewis, A.; Bumpus, J. A. Molecular Modeling of Environmentally Important Processes: Reduction Potentials. *J. Chem. Educ.* **2004**, *81* (4), 596.
(31) Bartmess, J. E. Thermodynamics of the Electron and the Proton. *J. Phys. Chem.* **1994**, *98* (25), 6420−6424.
(32) Stephens, L. I.; Mauzeroll, J. Demystifying Mathematical Modeling of Electrochemical Systems. *J. Chem. Educ.* **2019**, *96* (10), 2217−2224.
(33) Wang, S.; Wang, J.; Gao, Y. Development and Use of an Open-Source, User-Friendly Package to Simulate Voltammetry Experiments. *J. Chem. Educ.* **2017**, *94* (10), 1567−1570.
(34) Caceci, M. S.; Cacheris, W. P. Fitting Curves Data: The Simplex Algorithm Is the Answer. *Byte* **1984**, *9*, 340−348.
(35) Warren, J. J.; Tronic, T. A.; Mayer, J. M. Thermochemistry of Proton-Coupled Electron Transfer Reagents and Its Implications. *Chem. Rev.* **2010**, *110* (12), 6961−7001.
(36) Rochester, C. H. 855. A Comparison of the Acid Ionisation Constants of p-t-Butylphenol, o-t-Butylphenol, and 2,4-Di-t-Butylphenol in Water and Methanol. *J. Chem. Soc.* **1965**, 4603−4604.
(37) Litwinienko, G.; Ingold, K. U. Abnormal Solvent Effects on Hydrogen Atom Abstractions. 1. The Reactions of Phenols with 2,2-Diphenyl-1-Picrylhydrazyl (Dpph•) in Alcohols. *J. Org. Chem.* **2003**, *68* (9), 3433−3438.
(38) Freitas, K. H. G.; Fatibello-Filho, O. Simultaneous Determination of Butylated Hydroxyanisole (BHA) and Butylated Hydroxytoluene (BHT) in Food Samples Using a Carbon Composite Electrode Modified with Cu3(PO4)2 Immobilized in Polyester Resin. *Talanta* **2010**, *81* (3), 1102−1108.
(39) Pavitt, A. S.; Bylaska, E. J.; Tratnyek, P. G. Oxidation Potentials of Phenols and Anilines: Correlation Analysis of Electrochemical and Theoretical Values. *Environ. Sci. Process. Impacts* **2017**, *19* (3), 339−349.
(40) Yousofian-Varzaneh, H.; Zare, H. R.; Namazian, M. Thermodynamic Parameters and Electrochemical Behavior of Tetrafluoro- p -Quinone in Aqueous Solution. *J. Electrochem. Soc.* **2015**, *162* (8), G63−G68.
(41) Marenich, A. V.; Ho, J.; Coote, M. L.; Cramer, C. J.; Truhlar, D. G. Computational Electrochemistry: Prediction of Liquid-Phase Reduction Potentials. *Phys. Chem. Chem. Phys.* **2014**, *16* (29), 15068−15106.
(42) Namazian, M.; Norouzi, P. Prediction of One-Electron Electrode Potentials of Some Quinones in Dimethylsulfoxide. *J. Electroanal. Chem.* **2004**, *573* (1), 49−53.
(43) Gan, T.; Shi, Z.; Hu, D.; Sun, J.; Wang, H.; Liu, Y. Synthesis of Graphene Oxide-Wrapped Core−Shell Structured Carbon Sphere@Al2O3 as Electrode Material for Voltammetric Determination of Butylated Hydroxyanisole in Food Products. *Ionics (Kiel)* **2015**, *21* (10), 2959−2968.
(44) Bonin, J.; Costentin, C.; Louault, C.; Robert, M.; Routier, M.; Savéant, J.-M. Intrinsic Reactivity and Driving Force Dependence in Concerted Proton−Electron Transfers to Water Illustrated by Phenol Oxidation. *Proc. Natl. Acad. Sci. U. S. A.* **2010**, *107* (8), 3367−3372.
(45) Brett, C. M. A.; Maria, A. N. A.; Brett, O. *Electrochemistry: Principles, Methods, and Applications*; Oxford University Press: Oxford, 1993.
(46) Orlik, M. An Improved Algorithm for the Numerical Simulation of Cyclic Voltammetric Curves Affected by the Ohmic Potential Drops and Its Application to the Kinetics of Bis(Biphenyl)-Chromium(I) Electroreduction. *J. Electroanal. Chem.* **2005**, *575* (2), 281−286.
(47) Namazian, M.; Zare, H. R. Computational Electrode Potential of a Coumestan Derivative: Theoretical and Experimental Studies. *Biophys. Chem.* **2005**, *117* (1), 13−17.

https://doi.org/10.1021/acs.jchemed.1c01230
J. Chem. Educ. XXXX, XXX, XXX−XXX